Integrated control of electromechanical braking and regenerative braking in plug-in hybrid electric vehicles

Zhiguang Zhou

College of Mechanical and Vehicle Engineering,
Hunan University,
Yuelu District, Changsha City,
Hunan Province, 410082, China

and

Department of Electrical and Computer Engineering,
University of Michigan-Dearborn,
4901 Evergreen Road,
Dearborn, MI 48128, USA
E-mail: chinazhiguang@gmail.com

Chris Mi*

Department of Electrical and Computer Engineering,
University of Michigan-Dearborn,
4901 Evergreen Road, Dearborn, MI 48128, USA
E-mail: mi@ieee.org
*Corresponding author

Guixiang Zhang

College of Mechanical and Vehicle Engineering,
Hunan University,
Yuelu District, Changsha City,
Hunan Province, 410082, China
E-mail: zgx0828@sina.com

Abstract: This paper proposes the use of Electromechanical Brakes (EMB) in combination with regenerative braking in PHEV so braking force can be distributed to front and rear axles according to an optimal curve instead of a linear line. Therefore, more braking force will be distributed to front axle, which will offer more kinetic energy for regenerative braking. Fuzzy logic control is used to allocate braking force between regenerative braking and electromechanical braking. The paper also studies antilock braking control of EMB to maintain safety and stability of a vehicle using sliding-mode control with switching gain fuzzy adjusting.

Keywords: plug-in; HEV; hybrid electric vehicle; EMB; electromechanical brakes regenerative braking; frictional braking; sliding-mode control; fuzzy logic.

Reference to this paper should be made as follows: Zhou, Z., Mi, C. and Zhang, G. (2012) 'Integrated control of Electromechanical Braking and regenerative braking in plug-in hybrid electric vehicles', *Int. J. Vehicle Design*, Vol. 58, Nos. 2/3/4, pp.223–239.

Biographical notes: Zhiguang Zhou received the BS from Xiangtan University, China, in 2004 and the MS from Hunan University, China, in 2007. He is now a Doctoral Student of Hunan University, China. At present, he is doing some research at the University of Michigan-Dearborn as a Visiting Scholar. His research interests focus on the design, modelling and control of hybrid electric vehicle.

Chris Mi is an Associate Professor of Electrical Engineering at the University of Michigan, Dearborn. He received his BSEE and MSEE from Northwestern Polytechnical University, China, and his PhD from the University of Toronto, Canada. His research interests are in power electronics, hybrid electric vehicles, electric machines and renewable energy systems. He worked for General Electric Canada Inc. from 2000 to 2001. He is the recipient of numerous awards including the Distinguished Teaching Award and Distinguished Research Award from the University of Michigan, National Innovation Award and Government Special Allowance Award from China, and IEEE and SAE Awards. He is a Senior Member of IEEE and has more than 100 publications.

Guixiang Zhang received the BS from Hunan University, China, in 1979. She is now a Professor at the College of Mechanical and Vehicle Engineering, Hunan University. Her teaching and research interests are in the areas of mechanical transmission control and computer control technology. She has published more than 30 technical papers in mechanical transmission control and computer control areas.

1 Introduction

Hybrid and Plug–In Hybrid Electric Vehicles (PHEVs) offer significant fuel savings compared with conventional gasoline- and diesel-powered vehicles (Simpson, 2006). In HEV and PHEV, the braking force is coordinated between regenerative braking and frictional braking (Gao and Ehsani, 2001). Regenerative braking force is produced by the electric motor and the mechanical braking force is supplied by hydraulic brakes or air pressure brakes (Jonas, 2007). Regenerative braking is activated during coasting and decelerations to recapture a portion of the kinetic energy to charge the on-board energy storage system. This recaptured energy is then used to provide the electrical power required by the powertrain, as well as the vehicle accessory power loads during vehicle idle conditions (Gao et al., 1999). Because of the slow response of the traditional frictional brakes, coordination of the two braking systems has been proven to be extremely difficult, and the capability of recovering the maximum amount of energy during braking has been a challenge. On the contrary, EMB can control the braking torque precisely and quickly. To optimise the regenerative braking control so as to maximise the regenerative braking energy, we propose to use EMB to achieve the distribution of braking force to front and rear axes according to an optimal curve, also known as ideal curve or I-curve. We then use fuzzy logic control strategy to distribute the braking force between regenerative braking and frictional braking.

EMB can also realise anti-lock function during braking to maintain the safety and stability of the vehicle when it is on wet, snowy, or icy roads. The main difficulty arising in the design of braking control system is the high non-linearity of the system and the presence of disturbances and parameter uncertainties. A robust control methodology needs to be adopted to solve the problem. At present time, the commonly used method is logic threshold method based on experience, and plenty of experiments need to be carried out to obtain the threshold values (Chen, 1995). Other control strategies, such as PID control (Chen, 1995), fuzzy control (Chen and Liu et al., 2002; Li et al., 2001), neural network (Huang et al., 2003) and sliding-mode control (Wang et al., 2004; Ahn et al., 2009), have been studied for ABS control, but they are difficult to implement if real time in the real system.

Sliding-mode methodology has been adopted to design the observer since it is applicable to non-linear systems and has good robustness properties against disturbances, modelling inaccuracy and parameter uncertainties. However, the conventional sliding-mode control generates a discontinuous control action that has the drawback of producing high-frequency chattering, with the consequent excessive mechanical wear and passenger's discomfort. To reduce the vibrations induced by the controller, fuzzy logic control is used to adjust the switching gain of sliding-mode control. Simulation results indicate that the chattering is greatly decreased.

2 Braking principle of PHEV with EMB

The architecture of the studied vehicle is a blended mode, front wheel drive, power-split PHEV as shown in Figure 1. The engine and motor can supply power at the same time or alone under different driving conditions, according to power management algorithms. To convert kinetic energy to electrical energy, the system uses the motor as a generator. The generator produces a torque to resist the rotation of the wheels, providing brake force needed to slow the vehicle. The generator can also produce electricity with the excessive power from the engine, so as to adjust the operation area of the engine to keep the engine operating in the high-efficiency region. Four EMBs are installed in the vehicle, which can supply braking torque to all four wheels independently. In addition, the EMB also provides the anti-lock braking function. The EMBs communicate with the brake controller by FlexRay or CAN bus.

In a regular HEV, braking torque is a combination of regenerative braking, frictional braking and frictional torque of the engine. Since the engine frictional torque will decrease the regenerative amount, to obtain more regenerative energy, in this paper, engine will be disconnected at the time of braking. The main parameters of the PHEV are shown in Table 1.

Table 1 Parameters of PHEV

Component	*Rating*
Engine	5.7 L 257 kW
Motor	65 kW
Generator	65 kW
Battery pack	Lithium-ion battery, 10 kWh, 300 V
Vehicle gross weight	3298 kg

Figure 1 Architecture of PHEV (see online version for colours)

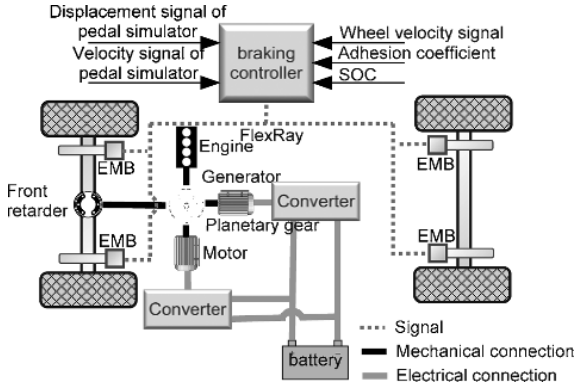

In this paper, a non-linear model of the vehicle is adopted (Yang et al., 2009). The vehicle is modelled as a rigid body, and only longitudinal motion is considered. The difference between the left and right tyres is neglected, making reference to a so-called bicycle model. The lateral, yawing, pitch, and roll dynamics, as well as actuator dynamics, are also neglected.

3 EMB System

The EMB system replaces the conventional hydraulic system with an electromechanical system, a type of Brake By Wire (BBW) system, which employs an EMB module as the braking module for each wheel. The EMB system is able to provide a large braking torque, using only a small brake pedal reaction force and a short pedal stroke (Ahn et al., 2009).

The EMB system consists of the EMB controller, motor, deceleration and motion conversion device (Line et al., 2008). The EMB controller is used to control the output torque of the motor. The requirement of EMB system to the motor is that the machine can produce large torque at low speed, both Switched Reluctance Motor (SRM) and permanent magnetic motor are candidates for EMB system. EMB system would produce large heat during braking, which will cause the temperature to rise and the demagnetisation phenomenon will occur when the permanent magnetic motor stays at high temperature for a certain time. So, we select the SRM as our implementation device. Another reason is the robustness and simplicity of SRM. The deceleration device has the function of deceleration and increasing mechanical torque. The motion conversion device is used to convert rotary motion into linear motion, so as to compress braking disc. The architecture of the proposed EMB is shown in Figure 2.

Figure 2 The architecture of the proposed EMB (see online version for colours)

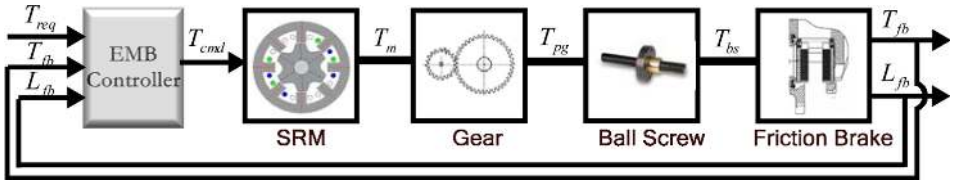

3.1 A mathematical model of EMB

Among the three most common SRMs, three-phase 6/4-pole SRM, four-phase 8/6-pole SRM and five-phase 10/8-pole SRM (Krishnamurthy et al., 2009), the three-phase 6/4-pole SRM produces large torque ripple and a five-phase 10/8 SRM is more complex and has high cost. Therefore, the four-phase 8/6-pole SRM is used in this paper as shown in Figure 3.

Figure 3 Structure of four 8/6 SRM (see online version for colours)

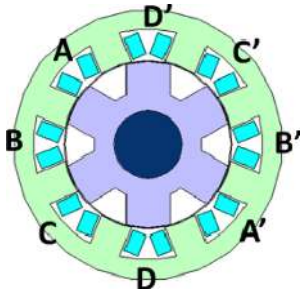

The rating of the four-phase 8/6-pole SRM used in this paper is 200W, 42V. Each SRM can supply as high as 13kN braking force.

Set the kth (k = 1, 2, 6) phase voltage, current, resistance, inductance, flux linkage and torque as u_k, i_k, R_k, L_k, ψ_k and T_k, respectively, rotor position angle is θ, rotor speed is ω, winding co-energy is W_m, moment of inertia is J, viscous friction coefficient is B and load torque is T_L. To simplify the calculation, inter-phase mutual inductance is neglected and interaction between phases produced by stator and rotor yoke saturation when more than two phases conducted is also not considered. The kth phase flux linkage equation of SRM can be described as

$$\psi_k = \psi_k\left(i_k, \theta\right) = L_k(i_k, \theta)\, i_k. \tag{1}$$

The kth phase winding voltage equation of SRM is represented by

$$u_k = R_k\, i_k + \frac{\mathrm{d}\psi_k}{\mathrm{d}t}. \tag{2}$$

Substituting equation (1) in equation (2), we can obtain

$$u_k = R_k\, i_k + \left(L_k + i_k \frac{\partial L_k}{\partial i_k}\right)\frac{\mathrm{d}i_k}{\mathrm{d}t} + i_k \frac{\partial L_k}{\partial \theta}\frac{\mathrm{d}\theta}{\mathrm{d}t}. \tag{3}$$

According to electromechanical energy conversion principle, the kth phase electromagnetic torque of SRM can be written as

$$T_k = \frac{\partial W_m\,(i_k, \theta)}{\partial \theta} = T_k\,(i_k, \theta). \tag{4}$$

SRM output electromagnetic torque stacked by each phase electromagnetic torque can be described as

$$T_e = \sum_{k=1}^{4} T_k\left(i_k, \theta\right). \tag{5}$$

Mechanical motion equation of SRM is given by

$$J\frac{\mathrm{d}\omega}{\mathrm{d}t} = T_e - B\omega - T_L \tag{6}$$

$$\frac{\mathrm{d}\theta}{\mathrm{d}t} = \omega. \tag{7}$$

The mathematical model of the actuator is (Yang et al., 2009)

$$\theta_s = \theta / i_d \tag{8}$$

$$S_n = \theta_m L_s / (2\pi) \tag{9}$$

$$T_{bs} = F_s L_s /(2\pi\eta_t). \tag{10}$$

In equations (8)–(10), θ_s is the rotating angle of screw, i_d is the deceleration ratio of decelerator, S_n is the shift distance of nut, L_s is the thread lead of screw, T_{bs} is the thread torque of screw, F_s is the axial working load of screw and η_t is the transmission efficiency.

The mathematical model of the brake is

$$T_{fb} = 2F_s\mu_f R_b. \tag{11}$$

In equation (11), T_{fb} is the braking torque of brake and μ_f is the friction coefficient between braking friction plate and braking disc.

3.2 Torque control strategy of EMB

The block diagram of the proposed braking torque control strategy is shown in Figure 4, where T_e^* is the required braking torque. In the paper, it is assumed that there is only two phases conducting at the same time, so after Torque Distribution Function (TDF), T_e^* is divided into T_i^* and T_j^* ($i, j = A, B, C, D$), which describes the sequence phase rotor torque. The TDF is shown in Figure 5, which can be realised easily (David, 2001). With T_i^* T_j^* and rotor position angle θ, through a look-up table, which contain the relationship among phase torque, rotor position angle and phase current, sequence phase current i_i^* and i_i^* and i_j^* ($i, j = A, B, C, D$) can be obtained. The relationship among torque, rotor position angle and current can be obtained by experiment, as shown in Figure 6. Then, hysteresis current control method is used to produce gating signal to control the power converter with the input parameters i_i^*, i_j^*, θ and rotor current i_m. The power converter will generate input voltage to SRM according to the gating signal. So rotor torque will be produced and transferred to the gear. Simulation result shown in Figure 7 illustrates that the control method used in this paper can satisfy the torque precision of braking systems.

Figure 4 Block diagram of braking torque control strategy

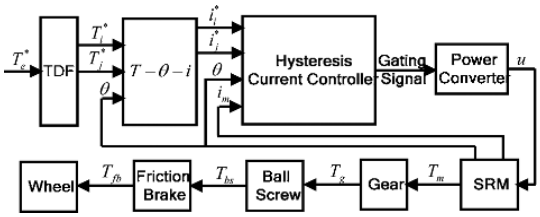

Figure 5 Torque distribution function (see online version for colours)

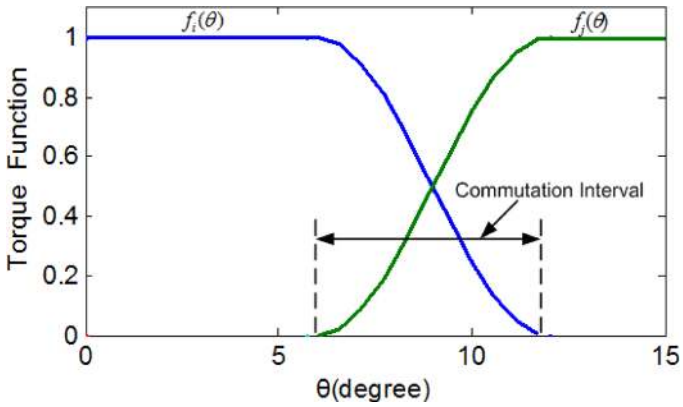

Figure 6 Relationship among torque, rotor position angle and current (see online version for colours)

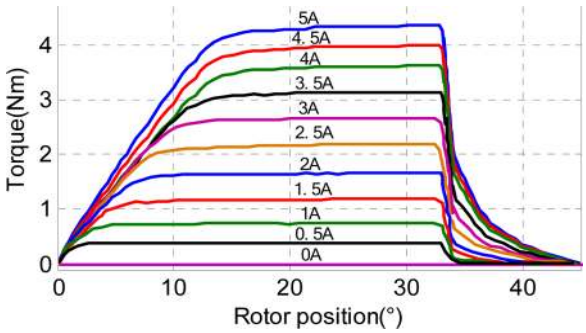

Figure 7 Actual torque follows required torque (see online version for colours)

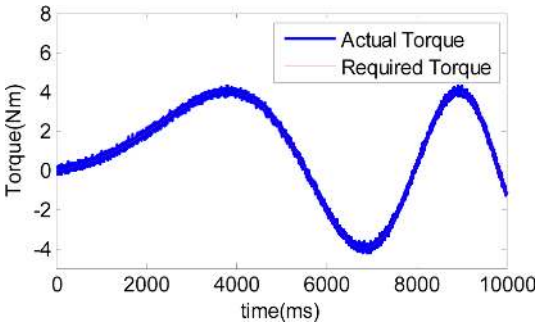

4 Integrated control of EMB and regenerative braking

The target of braking control system is to maximise regenerative energy while maintaining vehicle stability and safety. To achieve this goal, this paper uses an optimal or ideal curve (I-curve) to distribute the braking torque between front and rear axle, and then uses fuzzy logic to distribute braking torque between regenerative braking and friction braking in the front axle. Fuzzy-sliding mode control is used to avoid wheels being locked. The structure of braking control system is shown in Figure 8. In Figure 8 T_{xb_com} is the braking torque command from the driver. T_{xb_req} is the required braking torque after the adjusting of anti-lock braking controller. ΔT_{xb} is the adjusting quantity. T_{xb_f} and T_{xb_r} are braking torque distributed to front and rear axles, respectively. T_{xb_freg} and T_{xb_ffric} are braking torque distributed to regenerative braking and frictional braking, respectively. T_{xb_fl}, T_{xb_fr}, T_{xb_rt} and T_{xb_rr} are braking torque distributed to front-left, front-right, rear-left and rear-right wheels, respectively. ω_{fl}, ω_{fr}, ω_{rl} and ω_{rr} are angular speed of front-left, front-right, rear-left and rear-right wheels, respectively. v_x is the vehicle longitudinal speed.

Figure 8 Structure of braking control system

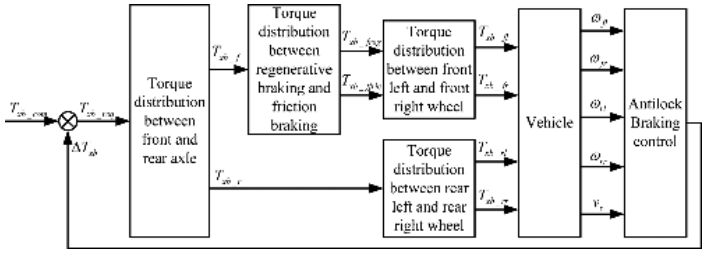

4.1 Torque distribution between front and rear axle

In conventional vehicles, the braking torque is difficult to be distributed to front and rear axle according to the I-curve because it is difficult to precisely control the hydraulic system. Traditional method distributes the total braking torque to front and rear axes according to some proportion. With EMB system, the braking torque can be precisely controlled with fast response time. Therefore, braking torque can be distributed between front and rear axle according to the I-curve as shown in Figure 9. To compare the distribution results from I-curve and from the traditional method, the torque distribution for the UDDS driving cycle is shown in Figures 10 and 11 for conventional and the proposed method, respectively. It can be seen that by using I-curve, more braking torque is distributed to the front axle, so it offers more possibility to capture more regenerative energy.

4.2 Torque distribution between regenerative braking and friction braking

In this paper, both regenerative and friction braking can supply braking torque to the front axle. It is important to properly distribute the front axle braking torque between regenerative and friction braking to maximise energy capture while maintaining safety of the vehicle and health operation of components (motor, inverter and battery). To achieve this goal, this paper uses fuzzy logic control strategy to distribute braking torque to

regenerative braking as much as possible under some constraints. The inputs of fuzzy logic controller are battery State Of Charge (SOC) and torque change ratio δ, which is defined as

$$\delta(t) = T_{xb_{req}}(t) \Big/ \left(T_{xb_{req}}(t-1) + \Delta T_{xb}(t)\right). \tag{12}$$

The output of fuzzy controller is regenerative braking factor β, so the regenerative braking torque T_{xb_freg} and friction braking torque in front axle can be obtained as

$$T_{xb\_freg} = \beta \cdot T_{xb\_f} \tag{13}$$

$$T_{xb\_ffric} = (1-\beta) \cdot T_{xb\_f}. \tag{14}$$

The membership function of input variables and output variable are shown in Figures 12–14, respectively. In Figure 12, TL means too low, L means low, M means middle, H means high and TH means too high. In both Figures 13 and 14, TS means too small, S means small, M means middle, L means large and TL means too large. According to engineering expertise and insight, the fuzzy control rules can be constructed as shown in Figure 15.

Figure 9 I-curve (see online version for colours)

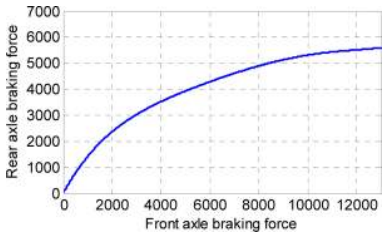

Figure 10 Braking torque distributed between front and rear axle using traditional method (see online version for colours)

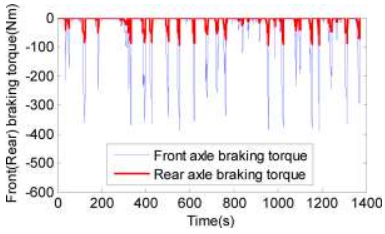

Figure 11 Braking torque distributed between front and rear axle using I-curve (see online version for colours)

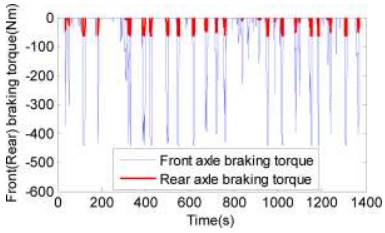

Under the precondition of distributing braking torque to front and rear axle, the results of distributing braking torque between regenerative braking and friction braking using look-up table method and using fuzzy logic control algorithm are shown in Figures 16 and 17, respectively. The parameters of the look-up table are obtained from vehicle simulation software Advisor 2002. It can be seen that more braking torque is distributed to regenerative braking with fuzzy logic control, which means more regenerative energy can be recovered. The regenerative energy obtained using the two methods are shown in Table 2.

Table 2 Regenerative energy using lookup table and using fuzzy logic control

Methods	*Regenerative energy*
Look-up table	971 kJ
Fuzzy logic control	1136 kJ

Figure 12 Membership function of SOC. TL – too low; L – low; M – Medium; H – high; TH – too high (see online version for colours)

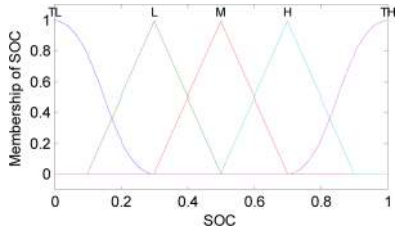

Figure 13 Membership function of δ. TL – too low; L – low; M – Medium; H – high; TH – too high (see online version for colours)

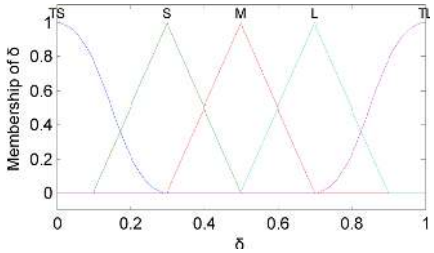

Figure 14 Membership function of β. TL – too low; L – low; M – Medium; H – high; TH – too high (see online version for colours)

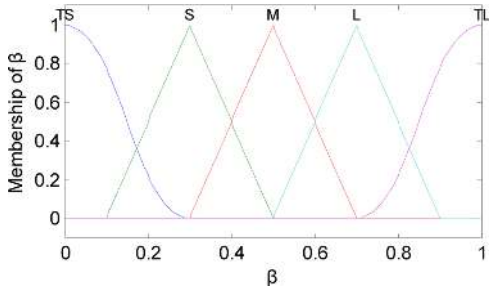

Figure 15 Rules of fuzzy logic control for braking torque distribution (see online version for colours)

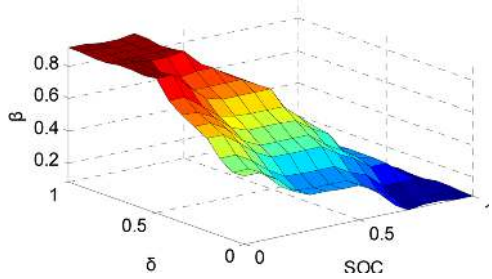

Figure 16 Braking torque distributed between front friction braking and regenerative braking using look-up table method (see online version for colours)

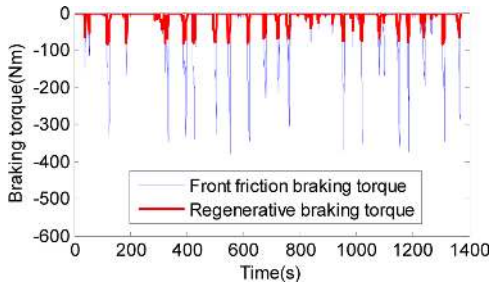

Figure 17 Braking torque distributed between front friction braking and regenerative braking using fuzzy logic control (see online version for colours)

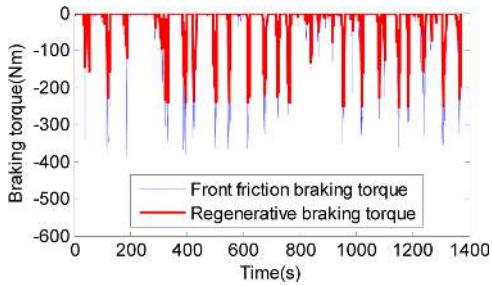

4.3 Anti-lock braking control

EMB system has the function of anti-lock braking. Vehicle braking system is a non-linear and time-variant system, and the vehicle model is uncertain. So, it is hard to build the precise mathematical model for the vehicle braking process. Sliding-mode control is insensitive to the changing of parameters of the control object. It has good anti-interference ability and good dynamic performance, and can response quickly. Therefore, it is suitable for both linear and non-linear systems. But, the algorithm of sliding-mode control has static error adjustment so it is hard to ensure the accuracy in static. It also has high instantaneous switching frequency on sliding-mode surface, which will affect the control precision of braking torque. To solve this problem, this paper uses fuzzy rules to do effective assessment for the switching gain according to sliding-mode

reaching condition to eliminate the interference, thus to eliminate chattering. The control diagram of vehicle braking system is shown in Figure 18. In the figure, s_{opt} is the optimal slip ratio; s is the real slip ratio calculated from the sensor signal of vehicle speed and wheel speed. By using sliding-mode control with switching gain fuzzy adjusting, the real slip ratio will track the optimal slip ratio, so as to ensure the vehicle braking system follows the optimal slip ratio.

Figure 18 Structure of fuzzy-sliding mode control

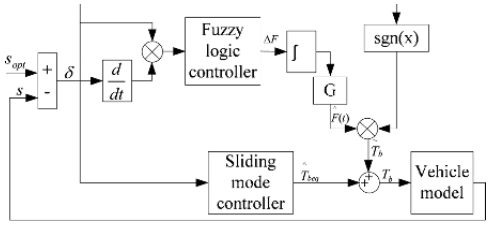

4.4 Design of sliding-mode controller

In vehicle EMB system, four wheels are controlled by using the same control method separately. To simplify the analysis, aerodynamic drag force and rolling resistance are neglected; the motion equations are described as follows:

Vehicle motion equation is

$$m\frac{\mathrm{d}v}{\mathrm{d}t} = -F_x(s). \tag{15}$$

Wheel motion equation is

$$J_\omega \frac{\mathrm{d}w}{\mathrm{d}t} = F_x(s)R - T_b(t). \tag{16}$$

Wheel longitudinal friction force is

$$F_x(s) = \mu(s)mg. \tag{17}$$

In equations (15) and (17), m is the one-fourth mass of total vehicle mass; v is the vehicle speed; $F_x(s)$ is the wheel longitudinal friction force; J_ω is the wheel inertia; ω is the wheel angle speed; R is the wheel radius; $T_b(t)$ is the braking torque; $\mu_{(s)}$ is the adhesion coefficient between wheel and road surface and g is the gravitational acceleration.

In the condition of braking, slip ratio can be defined as

$$s = \frac{v - v_\omega}{v} = \frac{v - \omega R}{v}. \tag{18}$$

In equation (18), v_ω is the wheel linear speed.

Taking derivative of both sides of equation (18), we can obtain that

$$\dot{s} = \frac{(1-s)\dot{v} - \dot{\omega}R}{v}. \tag{19}$$

Substituting equations (15)–(17) to equation (19), we can obtain that

$$\dot{s} = -\frac{\mu(s)mg}{v}\left[\frac{1-s}{m}+\frac{R^2}{J_\omega}\right]+\frac{T_b(t)R}{J_\omega v}. \tag{20}$$

Select the braking torque as the control object, and the control target is to find out the control rules, which can maintain the real slip ratio s oscillating around optimal slip ratio s_{opt}. Define the sliding-mode surface as

$$\delta(t) = s_e(t) = s_{opt} - s(t). \tag{21}$$

When the braking system moves along the sliding-mode surface, $\dot{\delta}(t) = 0$, so differentiate equation (21) and combine with equation (20), the equal control braking torque can be described as

$$\hat{T}_{beq} = \frac{J_\omega N\mu}{mR}(1-s) + N\mu R. \tag{22}$$

In equation (22), $N = mg$, which is the gravity of vehicle.

When braking system state is outside the sliding-mode surface, monitor control braking torque $\tilde{T}_b$ is added to ensure that the system state can reach at sliding-mode surface (Liu, 2005),

$$\tilde{T}_b = F(t)\cdot \mathrm{sgn}(\delta). \tag{23}$$

In equation (23), $\mathrm{sgn}(\cdot)$ is a sign function; $F(t)$ is used to compensate system interference to make sure the sliding mode exist condition can be satisfied. So, the output of control system is

$$T_b = \hat{T}_{beq} + \tilde{T}_b = \frac{J_\omega N\mu}{mR}(1-s) + N\mu R + F(t)\,\mathrm{sgn}(\delta). \tag{24}$$

In sliding-mode control law equation (24), switching gain $F(t)$ is the reason of causing chattering, because system interference is time variant, and to decrease chattering, $F(t)$ is also time variant. To eliminate the chattering caused by system interference, this paper uses fuzzy rules to estimate switching gain according to sliding-mode reaching condition.

4.5 Design of fuzzy logic controller

To eliminate the high-frequency chattering caused by time variable gain $F(t)$, the fuzzy logic rules can be designed as follows:

$$\text{If } \delta\dot{\delta} > 0, \quad \text{then increase } F(t) \tag{25}$$

$$\text{If } \delta\dot{\delta} < 0, \quad \text{then decrease } F(t) \tag{26}$$

With equations (25) and (26), fuzzy logic system can be designed about $\delta\dot{\delta}$ and $\Delta F(t)$. In this system, $\delta\dot{\delta}$ *is* the input and $\Delta F(t)$ is the output. Membership function of input and output of fuzzy logic system is shown in Figures 19 and 20. In both figures, NB means negative big, NM means negative middle, ZO means zero,

PM means positive middle and PB means positive big. The control rules are shown in Figure 21.

Using integration method to estimate the upper boundary of $\hat{F}(t)$,

$$\hat{F}(t) = G\int_0^t \Delta F dt. \tag{27}$$

In equation (27), G is the scale coefficient, $G > 0$

Figure 19 Membership function of input $\delta\dot{\delta}$ (see online version for colours)

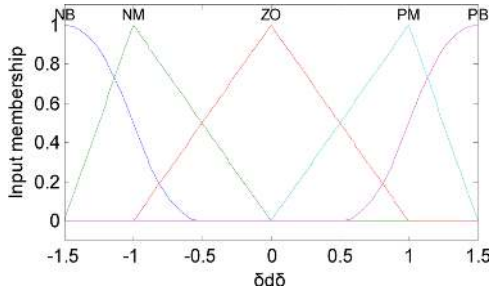

Figure 20 Membership function of output $\Delta F(t)$ (see online version for colours)

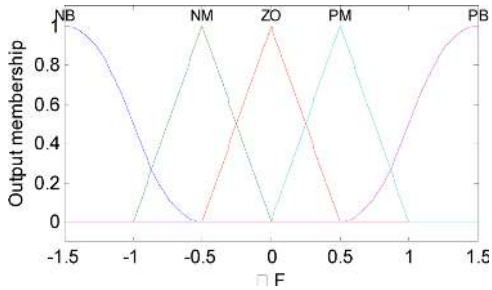

Figure 21 Fuzzy rules (see online version for colours)

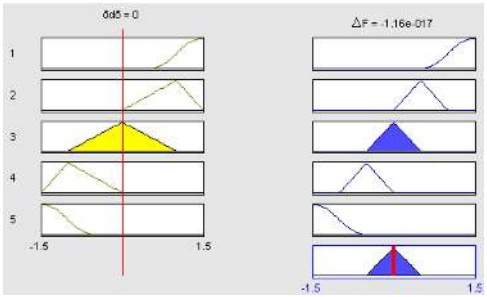

5 Analysis of simulation results

To test the braking performance under different braking conditions, a special drive cycle is constructed as shown in Figure 22. In the six phases, the acceleration is always

1.5 m/s^2, but the deceleration is varied, from −0.5 m/s^2 to −12 m/s^2. The required and actual deceleration is shown in Figure 23. It can be seen that when the deceleration is under −8 m/s^2, the braking system can supply required braking torque according to road adhesive force. But when the deceleration is greater than −8 m/s^2, because of the limit of road adhesive force, the actual deceleration cannot arrive at the required one. During the whole braking process, the slip ratio and adhesive coefficient are shown in Figures 24 and 25, respectively. From Figure 24, we can see that the slip ratio is always smaller than 1, which means that the wheels are never locked during the whole cycle. It also proves that the anti-lock braking control strategy used in this paper is feasible.

Figure 22 Constructed drive cycle (see online version for colours)

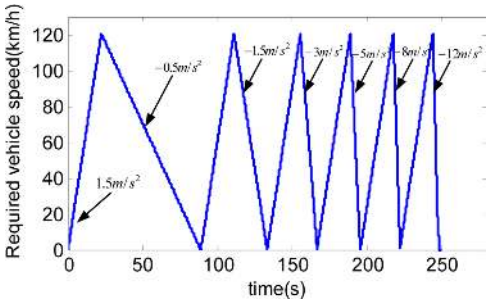

Figure 23 Required and actual deceleration (see online version for colours)

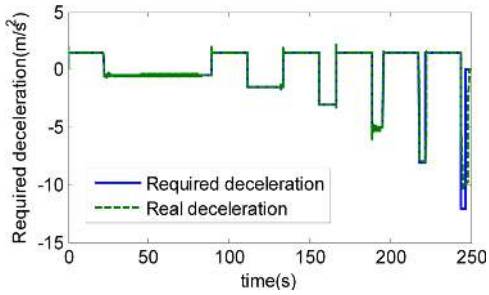

Figure 24 Slip ratio (see online version for colours)

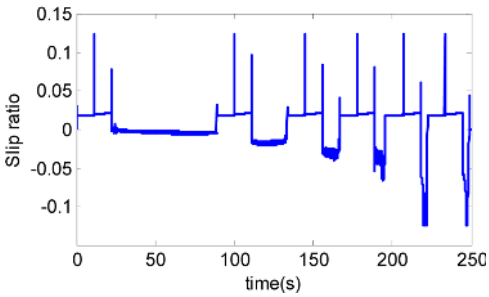

Braking torque distributed between front and rear axle and between regenerative braking and friction braking are shown in Figures 25 and 26, respectively. The results show that the braking distribution method used in this paper is feasible and reasonable.

Figure 25 Braking torque between front and rear axle (see online version for colours)

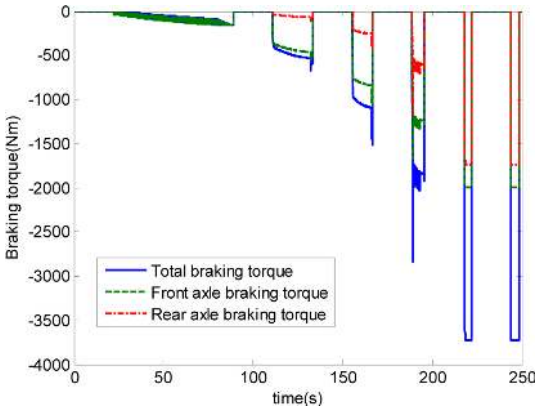

Figure 26 Braking torque between regenerative braking and friction braking (see online version for colours)

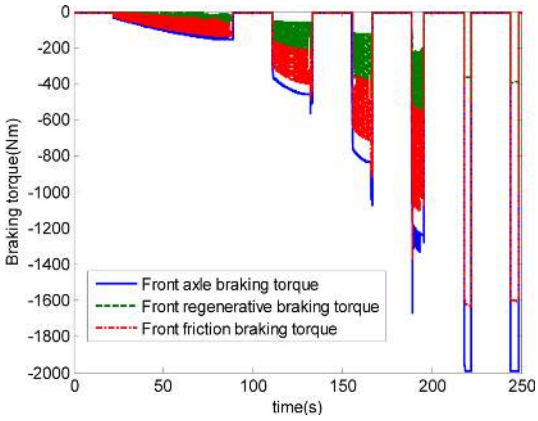

6 Conclusion

This paper proposed a coordinated control of regenerative braking and EMB in a PHEV. The main objective is to maximise the regenerative braking energy while maintaining the safety and stability of the vehicle during braking. To achieve this goal, from the aspect of hardware, considering the braking torque can be controlled precisely and quickly, EMB system is used as the frictional braking system. From the aspect of control method, first, an I-curve is used to distribute the total braking torque between front and rear axles so more braking torque is distributed to the front axis. It there offers more possibility to capture more regenerative energy. Second, fuzzy logic control is used to distribute braking torque between regenerative braking and friction braking on the front axis. Comparing with look-up-table-based method, fuzzy logic control strategy will distribute more braking torque to regenerative braking than to friction braking, which means more regenerative energy can be captured. To keep safety and stability of the vehicle, fuzzy-sliding mode control strategy is used to achieve the function of anti-lock braking. Standard driving cycles are used to test the performance of the control strategy. Simulation results indicate that the fuzzy-sliding mode control can keep the real slip ratio

following the optimal slip ratio closely and quickly, so the braking distance can be shortened and safety and stability of vehicle maintained.

References

Ahn, J.K., Jung, K.H. and Kim, D.H. (2009) 'Analysis of a regenerative braking system for hybrid electric vehicles using an electro-mechanical brake', *International Journal of Automotive Technology*, Vol. 10, No. 2, pp.229–234.

Chen, C. and Liu, J. (2002) 'The study of slip ratio based anti-lock brake system based on fuzzy control', *Journal of Wuhan University of Technology*, Vol. 24, No. 10, pp.50–53.

Chen, J. (1995) *Theory and Practice of Antilock Braking System*, Institute of Technology Press, Beijing.

David, I.J. (2001) *Switched Reluctance Motor Drives-Modeling, Simulation, Analysis, Design, and Applications*, CRC Press, Boca Raton, Florida, USA.

Gao, Y. and Ehsani, M. (2001) *Electronic Braking System of EV And HEV – Integration of Regenerative Braking*, Automatic Braking Force Control and ABS, SAE Technical Paper, 2001-01-2478, pp.1–7.

Gao, Y., Chen, L. and Ehsani, M. (1999) *Investigation of the Effectiveness of Regenerative Braking for EV and HEV*, SAE Technical Paper, 1999-01-2910, pp.1–7.

Huang, S-J.,Huang, K-S. and Chiou, K-C. (2003) *Development and Application of a Novel Radial Basis Function Sliding Mode Controller*, Mechatronics,Vol. 13, pp.313–329.

Jonas, H. (2007) 'Maximisation of brake energy regeneration in a hybrid electric parallel car', *Int. J. Electric and Hybrid Vehicles*, Vol. 1, No. 1, pp.95–121.

Krishnamurthy, P., Lu, W.and Khorrami, F. (2009) 'Robust force control of an SRM-based electromechanical brake and experimental results', *IEEE Transactions on Control Systems Technology*, Vol. 17, No. 6, pp.1306–1317.

Li, J. Yu, F. and Zhang, J. (2001) 'Fuzzy control of anti-lock braking system based on road automatic identification', *Transaction of Agricultural Machinery*, Vol. 32, No. 5, pp.26–29.

Line, C., Manzie, C. and Malcolm, C. (2008) 'Good. Electromechanical brake modeling and control: from PI to MPC', *IEEE Transactions on Control Systems Technology*, Vol. 16, No. 3, pp.446–457.

Liu, J. (2005) *MATLAB Simulation of Sliding Mode Control*, Tsinghua University Press, Beijing.

Simpson, A. (2006) 'Cost-benefit analysis of plug-in hybrid electric vehicle technology', *22nd International Battery, Hybrid and Fuel Cell Electric Vehicle Symposium and Exhibition (EVS-22)*, Yokohama, Japan, pp.1–15.

Wang, J., He, H. and Chen, Y. (2004) 'Control method of ABS based on adhesion coefficient – slip curve', *Vehicle Technology*, Vol. 6, pp.13–16.

Yang, K., Li, J. and Li, Y-d. (2009) 'Study of EBD/ABS based on electromechanical brake system', *Journal of System Simulation*, Vol. 21, No. 6, pp.1785–1788.